



Experimental Investigation and Comparison of a Decalin/Butylcyclohexane Based Naphthenic Bio-Blendstock Surrogate Fuel in a Compression Ignition Engine

Rodrigo Ristow Hadlich, Zhongnan Ran, Ruinan Yang, and Dimitris Assanis Stony Brook University

Ofei Mante and David Dayton RTI International

Citation: Ristow Hadlich, R., Ran, Z., Yang, R., Assanis, D. et al., "Experimental Investigation and Comparison of a Decalin/Butylcyclohexane Based Naphthenic Bio-Blendstock Surrogate Fuel in a Compression Ignition Engine," SAE Technical Paper 2022-01-0513, 2022, doi:10.4271/2022-01-0513.

Received: 26 Jan 2022

Revised: 26 Jan 2022

Accepted: 12 Jan 2022

Abstract

Many efforts have been made in recent years to find renewable replacements for fossil fuels that can reduce the carbon footprint without compromising combustion performance. Bio-blendstock oil developed from woody biomass using a reliable thermochemical conversion method known as catalytic fast pyrolysis (CFP), along with hydrotreating upgrading has the potential to deliver on this renewable promise. To further our understanding of naphthenic-rich bio-blendstock oils, an improved formulation surrogate fuel (SF), SF1.01, featuring decalin and butylcyclohexane naphthenic content was devised and blended with research-grade No.2 diesel (DF2) at various volume percentages. The blends were experimentally evaluated in a single-cylinder Ricardo Hydra compression ignition engine to quantify engine and emissions performance of SF1.01/DF2

blends. Injection timing events were varied from knock limit to misfire limit at the same operating conditions for all blends. A decrease in the engine power output was observed as the SF content was increased due to lower combustion efficiency, yielding slightly higher *CO* and *THC* emissions. Higher SF content also correlated with a significant decrease in the PM emissions. *NOx* emissions were minimal as they fell below detectable limits. A comparison is also presented between DF2 and previously published SF1/DF2 blends that featured only decalin as the naphthenic content. It was found that butylcyclohexane is more desirable from a combustion performance and emissions characteristic than decalin for the composition of the naphthenic content. A bio-blendstock oil of similar composition to the evaluated SF would be a good candidate for displacing fossil-derived heavy petroleum distillate fuels in engine applications.

Introduction

It is imminent that society will soon be forced to transition from fossil fuels to renewable energy sources due to its depletion and negative environmental impact. Biofuels are a promising solution to this problem as they are renewable and, depending on the quality, would not require modifications to current engine architecture and infrastructure associated to fuel distribution. There are also possible improvements that can be made in the environmental aspect using biofuels, such as ones derived from biomass [1-4], given that cultivating such biomass leads to removal of carbon dioxide (CO_2) from the atmosphere before being converted into fuel.

Such biofuels derived from biomass, and specifically waste biomass and other sources, are of particular interest because, contrary to first generation biofuels [5], they do not make use of resources that would otherwise be directed to the production of food [6-9]. However, these biofuels have certain

undesirable characteristics, that cause the fuel system to degrade and underperform over time [10-13]. To target these issues there are processes that can be used to improve the quality of the fuel by removing undesirable compounds from its composition, processes such as catalytic fast pyrolysis (CFP), hydrodeoxygenation (HDO), and esterification. Specifically, CFP is used to improve physicochemical characteristics and reduce contents of acids, oxygenates, and other undesirable compounds [14, 15], and Hydrotreating (HT) is used to reduce oxygen content [16]. A bio-blendstock derived from woody biomass using the CFP and HT pathway was produced at a pilot-scale catalytic pyrolysis unit [17]. The fuel produced was designed to present low aromatic and high naphthenic content to reduce soot formation, as it has been demonstrated that a higher aromatic content in the fuel leads to higher levels of soot [18, 19].

To develop large enough volumes required for engine testing, Ran et al. [20] have created a surrogate fuel from pure compounds that closely mimics the thermophysical and

compositional characteristics of the naphthenic bio-blendstock oil and conducted engine experiments to evaluate the performance of the fuel. Although the results presented demonstrate the feasibility of this fuel to be used as a drop-in replacement to conventional diesel, the fuel still contained low levels of aromatics in its composition. This motivated the production of a new bio-blendstock with an even lower aromatic and higher naphthenic content, and a surrogate fuel made from pure compounds was produced to simulate the behavior of the actual bio-blendstock. In this new surrogate fuel, the aromatic content that was present in the work of Ran et al. [20] was entirely replaced with naphthenic compounds.

Therefore, in this study an improved surrogate fuel, SF1.01, with high (69% by wt.) naphthenic content was produced and blended with research grade No.2 diesel in different percentages. Engine experiments using a single cylinder research diesel engine were conducted to evaluate the combustion performance and perform the emission characterization of the surrogate fuel/blends. The results were compared to baseline research-grade No.2 diesel fuel and the previously characterized surrogate fuel, SF1, by Ran et al. [20].

Methodology

Surrogate Fuel Composition and Mixing

The fuel used for engine testing is a surrogate fuel made from pure chemical compounds in a way that most closely simulates the composition of the bio-blendstock. Table 1 presents the weight percentage distribution of the surrogate fuel composition, as well as the level of purity of each compound. It also displays the chemical composition of the surrogate fuel (SF1) tested by Ran et al. [20] for comparison purposes.

The chemicals were purchased from Sigma Aldrich and Fischer Scientific and mixed in-house using two high accuracy scales 0-200g and 0-2000g and a variety of pipettes and spatulas of different sizes were used in the handling and precise measurement of the chemical compounds being added to the mixture. Figure 1 is included for a visualization of the mixing process.

Engine Experimental Setup

The engine used to perform the experiments reported on this paper is a light-duty 1.7L production General Motors Circle-L

FIGURE 1 Chemical compounds and tools used during fuel mixing process.



engine head attached to a Ricardo Hydra research engine block with further details provided previously by Ickes [21], Hariharan et al. [22] and Ran et al. [20]. Three of the four cylinders were deactivated to develop a functional single-cylinder production cylinder head. Details about the engine geometry as well as timing of valve events which have been modified for our research requirements, are presented in Table 2.

For complete analysis of engine performance and emission characteristics, thermocouples, pressure gauges, and heaters are inserted in key locations of the coolant, oil, intake, and exhaust systems. A 30hp DC dynamometer is used to control the engine speed and measure the torque and power

TABLE 2 Engine parameters of the single-cylinder research engine.

Stroke	79 mm
Bore	86 mm
Connecting Rod	160 mm
Compression Ratio	15.1:1
Number of Valves Per Cylinder	4
Piston Pin Offset	0.6 mm
Exhaust Valve Opening (EVO)	122° ATDC
Exhaust Valve Closing (EVC)	366° ATDC
Intake Valve Opening (IVO)	354° BTDC
Intake Valve Closing (IVC)	146° BTDC

TABLE 1 Surrogate fuel composition by weight percentage.

Label	Chemical Compound	SF1.01 (Wt.%)	SF1 (Wt. %) Ran et al. [20]	Purity/Description
A	4-Methylphenol	5.0	5.0	≥99%, FG
B	Phenanthrene	1.8	3.5	98%
C	Tetralin	12.5	25.0	Anhydrous, 99%
D	Decalin	34.6	55.0	Anhydrous, ≥99%
E	Butyl-cyclohexane	34.6	0.0	>99%
F	Octadecane	7.0	7.0	99%
G	Decane	4.5	4.5	For synthesis

output from the engine. Kistler pressure transducers are used to measure the intake, cylinder, and exhaust pressures at every 0.1 crank angle degrees (CAD). The position of the crankshaft is measured using a Kistler crankshaft encoder, also with 0.1 CAD accuracy. An ECM Lambda CAN module is used to measure the oxygen content of the exhaust gas and calculate the air/fuel ratio. The exhaust gas is also sampled using a Horiba MEXA emissions bench to measure the concentration of carbon monoxide (CO), carbon dioxide (CO_2), nitrogen oxides (NO_x), and total hydrocarbons (THC) with further details previously disclosed [23, 24]. A TSI Nanoparticle Emission Tester (NPET) 3795-HC is used to measure the particulate matter (PM) number concentration emissions.

The signals from all sensors mentioned are collected by a data acquisition system composed by National Instruments chassis and modules, which are connected to a computer that employs an in-house LABVIEW code. This code is used for collecting the sensor signals, as well as processing the data into useful parameters and displaying it in real time for the user. It is also through this code that the user controls the engine parameters for a given experiment. A schematic and pictorial representation are shown in Figures 2 and 3, respectively, to visualize the provided facility information.

Uncertainty Quantification

Uncertainty quantifying is both necessary and an important component of experimental work in order to best understand the quality of the collected data. The errors and uncertainties of the experimental setup have been listed in the works of Ran et al. [20] and can be extended to this body of work, given that the same experimental facility was utilized. The uncertainties associated with the fuel blend compositions are due to uncertainties in the mixing and blending processes have been quantified and detailed in this section.

The first step of the fuel preparation process requires one to mix all the pure chemical compounds that are needed. The desired fuel compositions are determined on a percent weight

FIGURE 2 Single-cylinder engine schematic adapted from Ran et al [20].

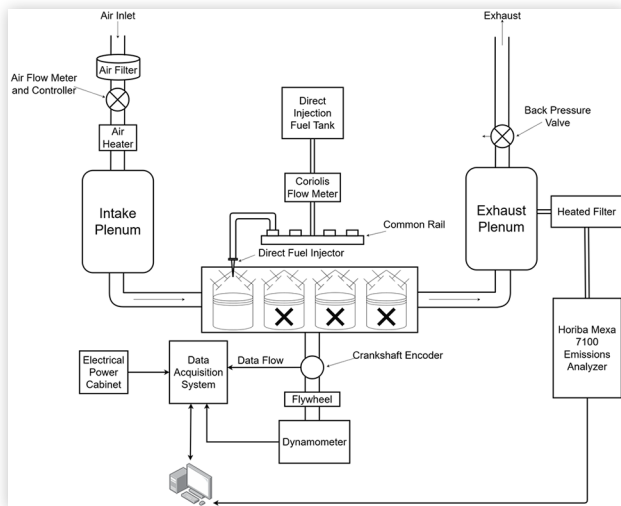
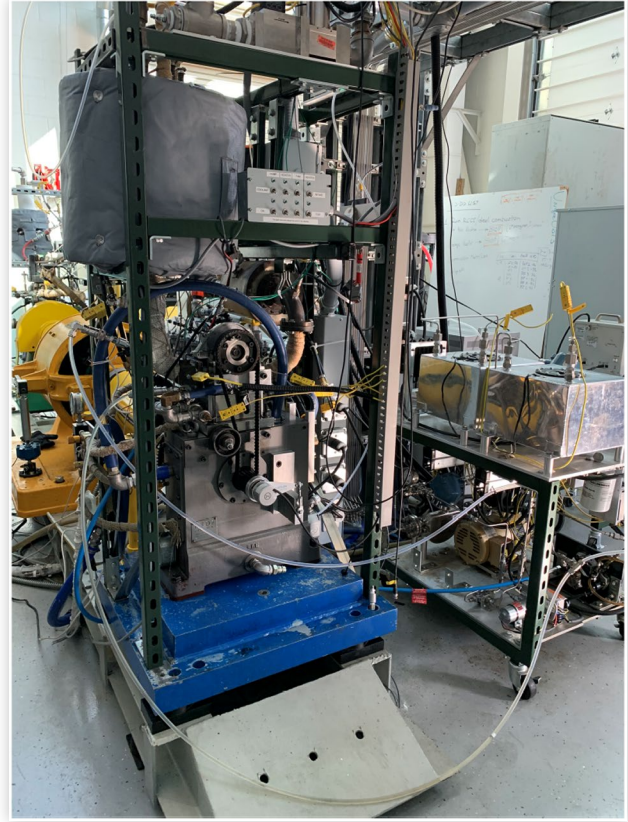


FIGURE 3 Diesel Hydra single-cylinder research engine at the Advanced Combustion & Energy Systems Laboratory of Stony Brook University.



(Wt. %) basis, so the measurements can be made on a weight basis. Two different scales are used for this process: Ohaus CL201 with a 0-200g range, and Ohaus CL2000 with a 0-2000g range. The total uncertainty of the measurement acquired using these scales can be determined by accounting for the resolution, precision, and accuracy errors using the Root Sum of Squares (RSS) methodology. These individual uncertainty values are given by the manufacturer and are presented in Table 3. The calculations of the total uncertainty for models CL201 and CL2000 are shown below for reference:

$$\begin{aligned} Err_{Scale_CL201} &= \sqrt{Err_{acc_CL201}^2 + Err_{res_CL201}^2 + Err_{rep_CL201}^2} \\ &= \sqrt{0.1^2 + 0.1^2 + 0.1^2} = 0.173 \text{ grams} \end{aligned} \quad (1)$$

$$\begin{aligned} Err_{Scale_CL2000} &= \sqrt{Err_{acc_CL2000}^2 + Err_{res_CL2000}^2 + Err_{rep_CL2000}^2} \\ &= \sqrt{1^2 + 1^2 + 1^2} = 1.73 \text{ grams} \end{aligned} \quad (2)$$

Fuel batch sizes of 2.5L were prepared for SF1 and SF1.01 surrogate fuels, featuring a cumulative density of 0.84 g/ml, and thus yielding 2100g of total mass for both surrogate fuels.

The CL201 scale is preferred, when possible, due to its higher precision, however, the required weight of some of the chemical compounds exceeded the upper limit of this scale, and thus the CL2000 needed to be used for such cases. Based on the Wt. % of each compound, it was concluded that the larger range CL2000 scale needed to be used when measuring

TABLE 3 Values of uncertainty on scale measurements.

Model	CL201	CL2000
Resolution (res.) (g)	0.1	1
Precision (pre.) (g)	0.1	1
Accuracy (acc.) (g)	± 0.1	±1

amounts of tetralin and decalin for SF1, and tetralin, decalin, and butylcyclohexane for SF1.01, respectively. The remaining measurements could be made using the higher precision CL201 scale. Finally, the total uncertainty in the mixing processes can be calculated using the RSS methodology to add the mixing uncertainty associated with each compound required. The procedure is described by the equation below:

$$Err_{mix_mass_SF} = \sqrt{\sum \left[\frac{Err_{Scale}}{Comp_{mass}} \right]^2} \quad (3)$$

where Err_{Scale} is the error associated with the scale used for the measurement of a compound, and $Comp_{mass}$ is the mass of the compound that was measured to compose, in-part, the surrogate fuel. The summation symbol signifies the sum of the squares of scale error divided by compound mass for all compounds that are required for a given surrogate fuel. The calculation of the mixing error of SF1.01 can then be calculated as follows:

$$Err_{mix_mass_SF1.01} = \sqrt{\left[\frac{0.173g}{105g} \right]^2 + \left[\frac{0.173g}{37.8g} \right]^2 + \left[\frac{1.73g}{262.5g} \right]^2 + \left[\frac{1.73g}{726.6g} \right]^2 + \left[\frac{1.73g}{726.6g} \right]^2 + \left[\frac{0.173g}{147g} \right]^2 + \left[\frac{0.173g}{94.5g} \right]^2} \quad (4)$$

$$Err_{mix_mass_SF1.01} = 0.0091 = 0.91\% \quad (5)$$

The same procedure can be applied to the formulation of SF1 to yield a total compositional mixing uncertainty of 0.51%.

The second part of the fuel preparation process requires one to blend the surrogate fuel with research-grade No.2 diesel in different concentrations. The uncertainty associated with this process comes from the volume resolution on the graduated cylinder that is used as well as the accuracy error of the graduated cylinder itself, which is taken to be 1% of the full-scale measurement. For measurements using the graduated cylinder, the height of the liquid in the is judged by sighting the bottom of the meniscus, ensuring that it is observed with eyes leveled with the liquid height to avoid parallax error.

A 3.0L batch size was needed for each blend, so a graduated cylinder of 1L volume was determined to be the appropriate size. The increments of the markings on the cylinder are 10ml, which dictates that the reading error is ±5ml for each reading given that the level can fall between two demarcations. For each one of the blends, four measurements were required to reach the total of 3L, due to the difference between batch size and the capacity of the graduated cylinder used for the measurements. The RSS methodology can once again be used to calculate the total uncertainty for each measurement:

$$Err_{mix_vol} = \sqrt{Err_{acc_grad_cylinder}^2 + \left[\frac{Err_{res_grad_cylinder}}{measured_vol} \right]^2} \quad (6)$$

where $Err_{acc_grad_cylinder}$ is the accuracy error on the graduated cylinder, $Err_{res_grad_cylinder}$ is the resolution error of the graduated cylinder, and $measured_vol$ is the volume measured on the measurement at hand. As an example, the uncertainty for a 900ml measurement using graduated cylinder can be determined as:

$$Err_{mix_vol_900ml} = \sqrt{0.01^2 + \left[\frac{5ml}{900ml} \right]^2} = 0.0114 = 1.14\% \quad (7)$$

Using this procedure as well as the mixing uncertainty calculated for each surrogate fuel, the total uncertainty for a blend can be calculated using the following method:

$$Err_{Blend} = \sqrt{\sum_{i=1}^n [Err_{mix_mass_SF}^2 + Err_{mix_vol_i}^2] + \sum_{j=1}^m Err_{mix_vol_j}^2} \quad (8)$$

where i and n are associated with surrogate fuel measurements, and j and m are associated with DF2 measurements. Moreover, n is the number of surrogate fuel measurements required to reach the SF content of the blend, $Err_{mix_mass_SF}$ is the mixing mass error of the surrogate fuel used in the i^{th} measurement, $Err_{mix_vol_i}$ is the volume reading error of the i^{th} measurement, m is the number of DF2 measurements required to reach the DF2 content of the blend, and $Err_{mix_vol_j}$ is the volume reading error of the j^{th} measurement. Using this formula, the total uncertainty of a 3L blend of 10% SF1.01 and 90% DF2 can be calculated as follows, respectively:

$$Err_{Blend_10\%_SF1.01_90\%_DF2} = \sqrt{Err_{mix_mass_SF1.01}^2 + Err_{mix_vol_300ml}^2 + [2 * Err_{mix_vol_1000ml}^2] + Err_{mix_vol_700ml}^2} \quad (9)$$

$$Err_{Blend_10\%_SF1.01_90\%_DF2} = \sqrt{0.0091^2 + 0.0194^2 + 0.0091^2} = 0. \quad (10)$$

This same procedure can be applied to 30% and 50% blends of SF1.01 and also to 10% and 30% blends of SF1. The blending error of pure DF2 can be considered zero since it was poured directly into the fuel tank and thus did not go through the blending process. The final results of this error analysis are summarized in [Table 4](#).

Experimental Procedure

The experimental procedure adopted for this work is of an injection timing sweep. Parameters that were held constant include the injection pressure at 550 bar, the injection duration so that the fuel-air equivalence ratio, ϕ , was constant at 0.25, and the air intake valve was fully open, providing a constant

TABLE 4 Total blending error of surrogate fuel blends.

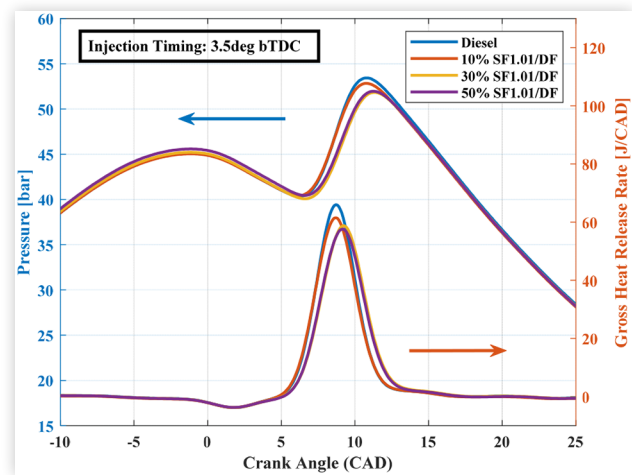
Blend Composition	Total blending error (%)
0% SF1 - 100% DF2	0
10% SF1 - 90% DF2	2.84
30% SF1 - 70% DF2	5.48
0% SF1.01 - 100% DF2	0
10% SF1.01 - 90% DF2	2.94
30% SF1.01 - 70% DF2	5.54
50% SF1.01 - 50% DF2	2.86

flow of air at ambient pressure and temperature. The injection timing was chosen as the varying parameter, and it ranged from knock limit to misfire limit in increments of 1 CAD. The same procedure was repeated for pure research-grade No.2 diesel and three surrogate fuel (SF)/diesel blends at 10, 30, and 50% SF content by volume (blends are labeled SF1.01/DF10, SF1.01/DF30, and SF1.01/DF50, respectively).

Results and Discussion

Performance and Emissions of SF1.01

Cylinder Pressure and Heat Release Rate The pressure inside the cylinder during a combustion cycle is perhaps the most important information collected as it is from this data that many of other performance parameters are calculated. It is also important to observe the heat release rate of the combustion process as it represents the rate at which fuel is converted to heat and contains information that helps better understand the behavior of the pressure traces. [Figure 4](#) is a plot containing both the pressure and the gross heat release curves with respect to crank angle degree (CAD) position for all blends at the same injection timing of 3.5° before top dead center (bTDC). Pure diesel has the earliest and highest peak in the heat release curve, meaning that once the fuel is injected in the cylinder it takes the least amount of time to mix with air and ignite, leading to more heat being released in a short period of time. Due to this heat release profile, it can also be observed in this figure that the peak highest pressure is achieved by pure diesel, and it decreases as the concentration of SF1.01 in the blend increases. Notably, higher cylinder pressures, within reason, can be desirable from a performance standpoint as they can increase the work being done on the piston and thus increasing the torque generated by the crankshaft. Higher heat release rates, again within reason, can also be beneficial as they can allow for a faster and potentially more complete combustion event to occur. A notable trend seen in [Figure 4](#), is that the peak cylinder pressure decreases with increasing SF fuel blend content. The reason for this observed behavior is due to the cetane number correspondingly decreasing with increasing SF1.01 content, which ultimately leads to a slight increase in the ignition delay period and thus the longer burn durations and the lower cylinder pressures observed.

FIGURE 4 Pressure and gross heat release rate time histories.

Engine Load The gross indicated mean effective pressure, $IMEP_{gross}$, is a valuable parameter that can be utilized to measure an engine's capacity to produce work that is independent of engine displacement. [Figure 5](#) presents the $IMEP_{gross}$ with respect to fuel injection timing for the baseline diesel fuel and the three fuel blends studied during experiments. As shown in the figure, the trend for all blends, except for the baseline diesel fuel, is that the $IMEP_{gross}$ increases at first and reaches a peak value close to the middle of the start of injection (SOI) range, and then ultimately drops to the lowest value. This behavior is expected due to the fact that the combustion event produces knocking events at advanced injection timing points, while in the retarded injection timing points the combustion is near misfire limit. Intermediate SOI values produce the highest maximum $IMEP_{gross}$ values because combustion is optimally phased with the crank-slider mechanism transmission efficiency, thus achieving the highest thermodynamic conversion efficiency of the engine.

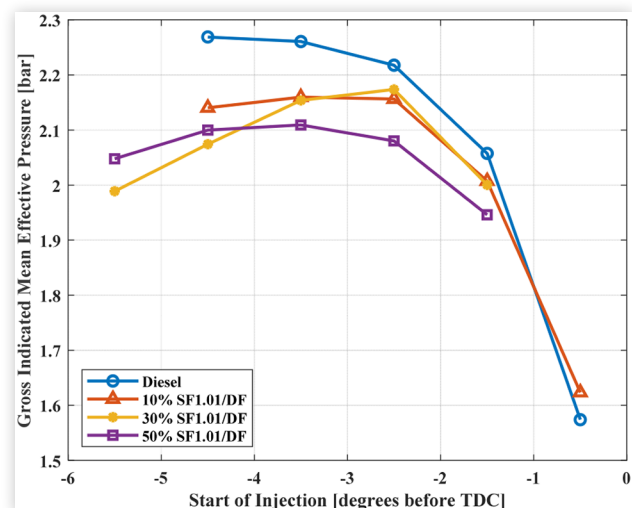
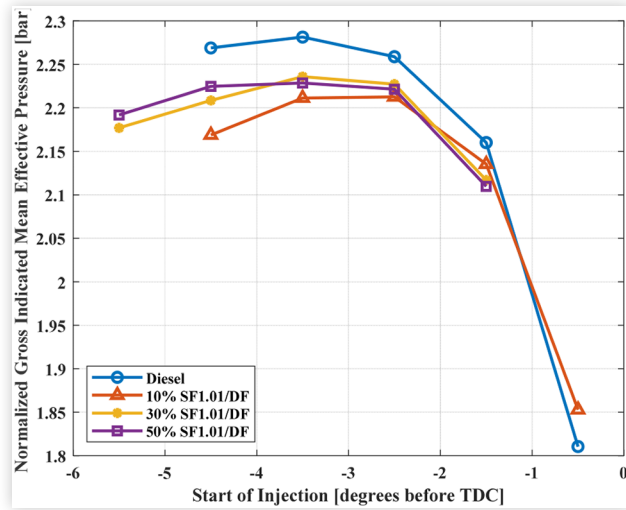
FIGURE 5 Engine $IMEP_{gross}$ with respect to injection timing.

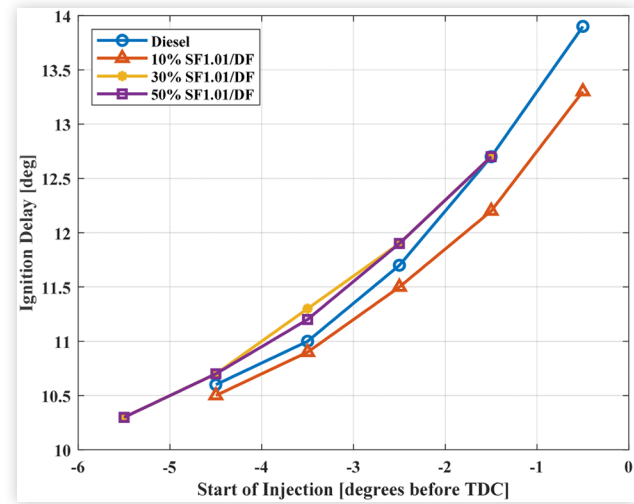
FIGURE 6 Engine normalized $IMEP_{gross}$ with respect to injection timing.



Another trend that can be observed is that the $IMEP_{gross}$ value decreases with increasing content of SF1.01. The highest $IMEP_{gross}$ was achieved by baseline diesel, followed by 10% SF1.01/DF, then 30% SF1.01/DF and lastly 50% SF1.01/DF. It is important to note here that throughout the experiments it was not possible to maintain the equivalence ratio at the desired operating point of $\phi = 0.25$, so part of the trend behavior observed here can be attributed to small variance in the equivalence ratio or ultimately the fuel energy input. To account for this discrepancy, the analysis was furthered to normalize the effects of the equivalence ratio. The normalized results are presented in Figure 6 and indicate that, although pure diesel still achieves the best performance, the SF1.01 blends have very close results, and increasing the SF1.01 content does not have as big of an impact on the blend performance as originally thought.

Ignition Delay and Combustion Efficiency The variation of ignition delay with respect to fuel injection timing for all the test fuels is shown in Figure 7. This parameter indicates how long the air-fuel mixture takes to ignite once the fuel is injected into the combustion chamber. From a combustion performance standpoint, a short ignition delay is desired because it leads to shorter burn durations, higher heat release rates, and higher peak cylinder pressure, which ultimately can lead to higher and cleaner energy conversion. As shown in this figure, the ignition delay of the engine decreases with advancing fuel injection timings. This is due to the increase in the cylinder peak temperature caused by the increased cylinder pressure as the fuel injection timing is advanced, which in turn reduces the physical ignition delay period. With respect to increasing blend composition content, a slight increase in the ignition delay is observed. It is, however, a mild increase (0.25-0.50 CAD) which does not lead to a significant impact in the overall performance. Ultimately, this indicates once again that a bio-blendstock oil with a similar formulation to the surrogate fuel SF1.01 may be a good candidate to be used as an alternative to fossil fuels

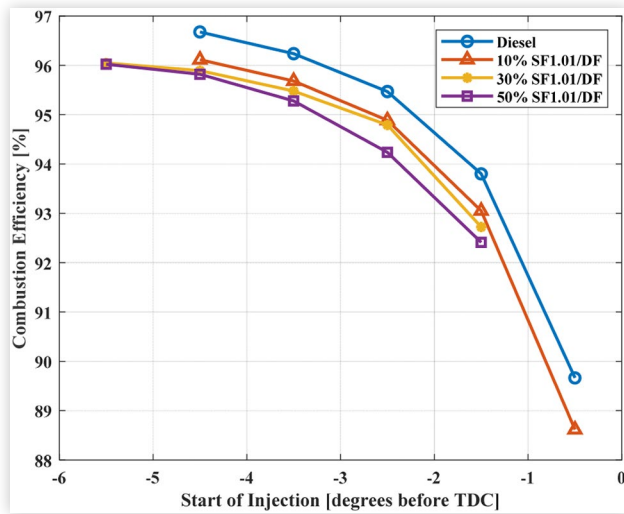
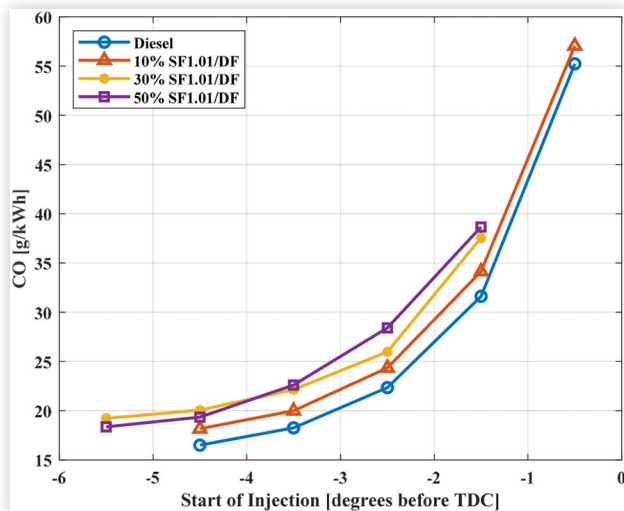
FIGURE 7 Ignition delay with respect to injection timing.



Combustion efficiency is a measure of how complete the combustion process is at converting fuel-air reactants into products. The combustion efficiency is calculated based on the exhaust emissions of CO and THC for conventional hydrocarbon fuels. The engine combustion efficiency with respect to the injection timing for the baseline diesel fuel and the three fuel blends is shown in Figure 8. The combustion efficiency increases as the injection timing is advanced from top dead center (TDC), and peaks at the earliest injection timing because the engine combustion temperature is the highest, as a result of the increased cylinder peak pressure. The fuel with the highest combustion efficiency is pure diesel, and it decreases as the surrogate fuel content increases, indicating that 50% SF1.12/DF has the lowest combustion efficiency. However, the maximum decrease in combustion efficiency observed is 1.5-2.0% which can be considered as minimal.

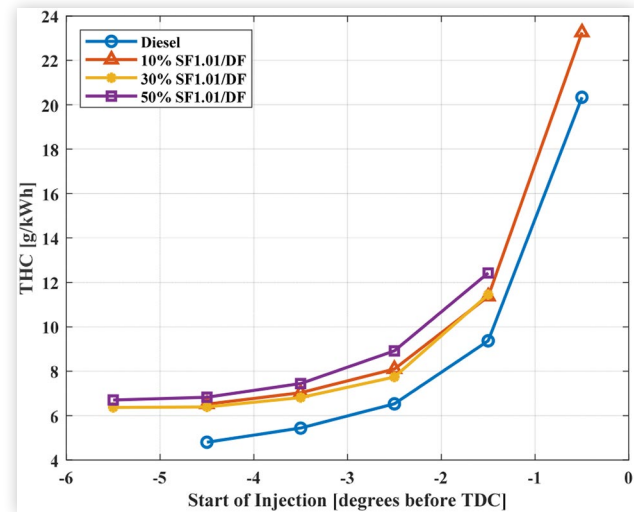
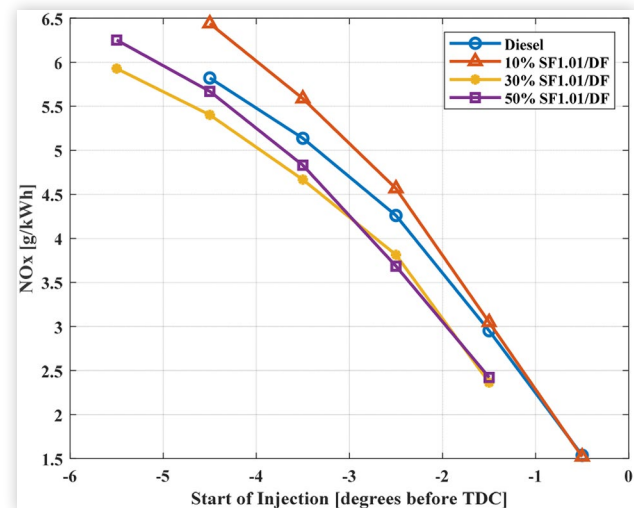
CO , THC and NO_x Emissions Figures 9 and 10 show, respectively, the indicated specific emissions of CO and THC with respect to injection timing for the baseline diesel fuel and the three fuel blends studied. The emissions of CO and THC are shown to be inversely proportional to the combustion efficiency since these gases are products of incomplete combustion of fuel. As the fuel injection timing is advanced from TDC, the emissions of CO and THC are both decreased until they reach their lowest point. Similarly, and in accordance with the combustion efficiency results observed, combustion with pure diesel resulted in the lowest levels of CO and THC emissions. The surrogate fuel blends resulted in higher emissions values, albeit most cases resulted in a minimal increase that could be easily handled by a modern aftertreatment system.

Figure 11 displays the indicated specific nitrogen oxide (NO_x) emissions as a function of fuel injection timing for the baseline diesel fuel and the three fuel blends evaluated. It is well known that the formation of NO_x emissions is dependent upon the engine bulk temperature and oxygen availability

FIGURE 8 Combustion efficiency with respect to injection timing.**FIGURE 9** CO emissions with respect to injection timing.

in the mixture. As shown in the figure, the NO_x emissions are increased as the fuel injection timing is advanced from TDC for all fuels studied. This can be attributed directly to the increased cylinder peak pressure and therefore an increased peak bulk temperature in the cylinder. From these experimental observations, increasing the blend content of SF1.01 into diesel fuel is not expected to have an appreciable difference in engine-out NO_x emissions. This validates, once again, that a bio-blendstock oil with a similar formulation to the surrogate fuel SF1.01 may be a good candidate to be used as an alternative to fossil diesel. Ultimately, the absolute value of NO_x emissions is extremely low because the overall peak bulk temperatures are also correspondingly very low.

Soot Emissions Figure 12 presents the effects of different surrogate fuel blends on the particle number concentration emissions of PM_{10} , particles having a smaller mean diameter

FIGURE 10 THC emissions with respect to injection timing.**FIGURE 11** NO_x emissions with respect to injection timing.

than $1 \mu m$. It is important to note that the device used to measure these emissions (TSI NPET 3795-HC) is optical-based and has a size range of 0.23 to $1 \mu m$, which is an appropriate range to capture even the smaller particles produced from the combustion chamber of an engine. Since soot particles are inversely proportional to the combustion efficiency, the first noticeable trend in the figure is that the soot emissions become larger as the start of injection is delayed closer to TDC. The other trend that can be observed is that the soot emissions become smaller as the SF1.01 blend ratio increases. This is a remarkable observation as baseline diesel has the largest value of soot particle number concentration followed by 10% SF1.01/DF, then 30% SF1.01/DF, and lastly 50% SF1.01/DF which demonstrated the best results. This may not be as apparent if looking at individual injection timings, but it is important to remember that the range of injection timings is different between the blends. For the 30% and 50% blends the injection timing is advanced to account for longer ignition delays. The soot emissions at knock limit and misfire limit becomes lower

as the SF content is increased, even though the injection timing at which knock and misfire are achieved varies.

Comparison of Performance of SF1 and SF1.01

The following section compares the performance of both generations of fuel blends, containing SF1 and SF1.01. Also included in the plots are the pure baseline diesel (DF2) data that were collected prior to testing the surrogate fuel blends. DF2 baseline experiments were performed before and after the experimental testing of the various fuel blends to ensure the hardware facility baseline behavior recovered and was not affected by any residual effects stemming from the introduction of the surrogate fuel compounds. The labels “DF2 (0% SF1)” and “DF2 (0% SF1.01)” identify the corresponding initial baseline DF2 data sets for the SF1 and SF1.01 fuel blend experiments, respectively.

Cylinder Pressure and Engine Load Figures 13 and 14 present the cylinder pressure traces at an injection timing of 3.5° before TDC and the trend in combustion efficiency, respectively, for all fuel blends of both SF1 and SF1.01. The cylinder pressure plot demonstrates that the performance of the SF1.01 blends is much closer to that of baseline diesel compared to the SF1 blends, and higher cylinder pressures are achieved by the new surrogate fuel. This can also be observed in Figure 14, and while it is true that increasing the surrogate fuel content leads to lower combustion efficiency for both generations of SF, it is noticeable that the efficiencies recorded for the SF1.01 blends are much higher than the SF1 efficiencies.

Combustion Duration Figure 15 shows the CA 10-90 of all fuel blends and both surrogate fuel generations. This parameter is an indicator of the duration of the combustion process once it has been initiated. A shorter burn is desired since a longer fuel burn process can lead to lower peak cylinder temperature and pressure conditions, which ultimately can

FIGURE 12 Soot emissions with respect to injection timing.

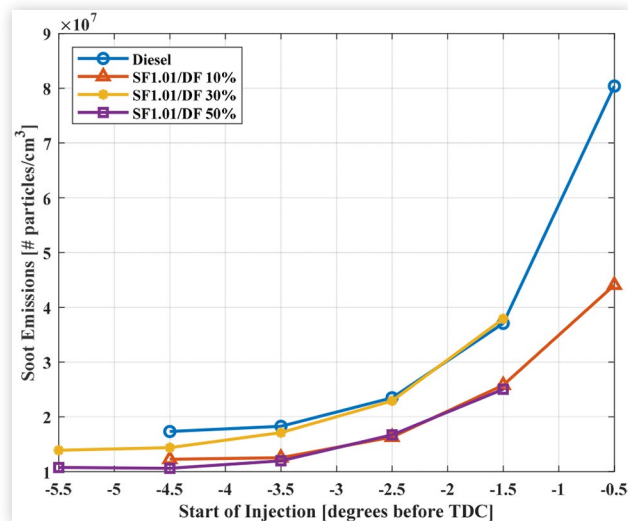
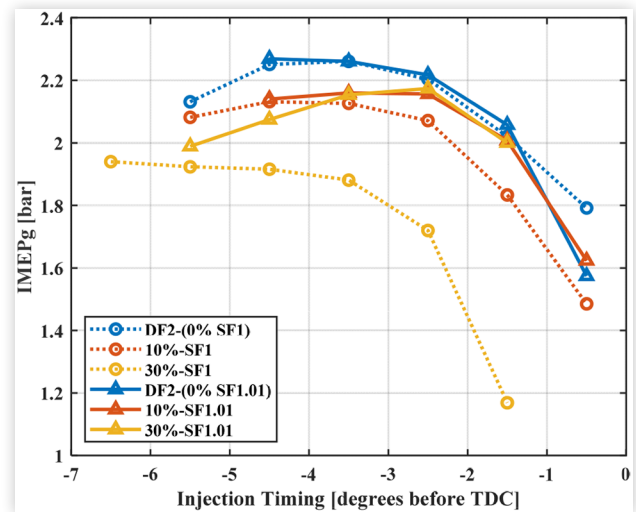


FIGURE 13 Comparison of IMEP_g of both blend generations with respect to injection timing. SF1 data courtesy of Ran et al. [20].



yield lower combustion efficiency and thus decreased energy conversion. Additionally, a shorter burn duration can also be advantageous as combustion phasing can be further varied to permit energy extraction to occur at a more advantageous crankshaft position. By analyzing Figure 15, it can be seen that the burn durations of blends containing SF1.01 are very close to that of pure diesel and lower than the SF1 blends. This behavior is in agreement with the behavior observed in the cylinder pressure and combustion efficiency.

CO and THC Emissions Figure 16 presents a comparison of the CO emissions for all blends of both fuel generations. The trend demonstrated is that the emissions are significantly lower for the SF1.01 blends, which are very close to the that of pure diesel. A similar behavior can be seen in Figure 17,

FIGURE 14 Comparison of combustion efficiency of both blend generations with respect to injection timing. SF1 data courtesy of Ran et al. [20].

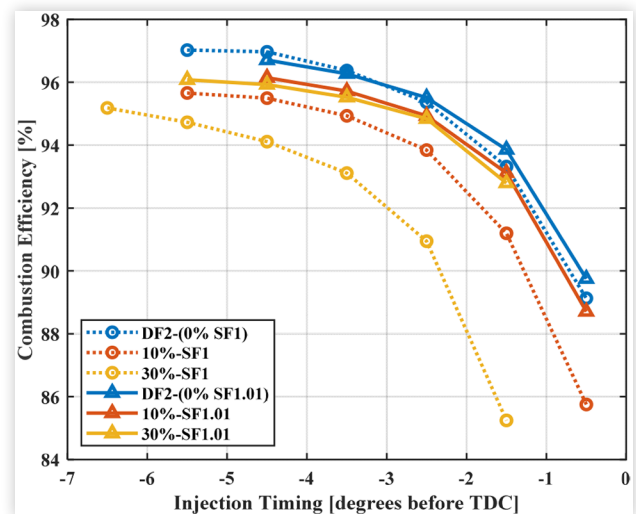


FIGURE 15 Comparison of burn duration (CA 10-90) of both blend generations with respect to injection timing. SF1 data courtesy of Ran et al. [20].

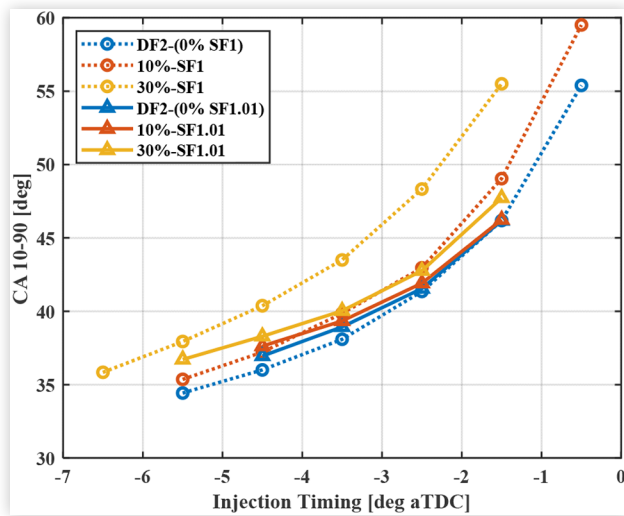
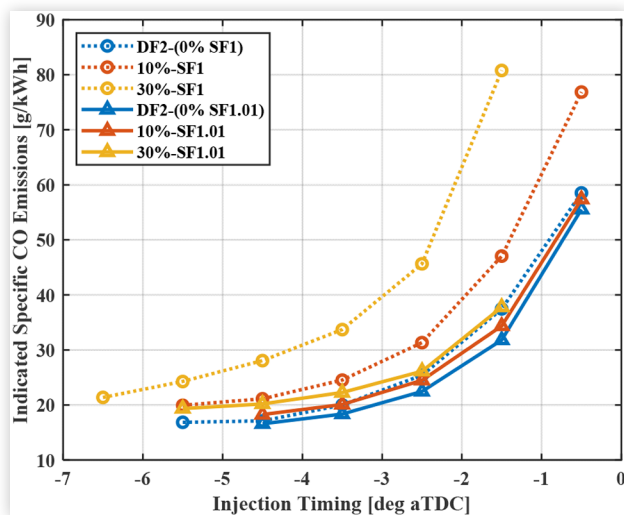


FIGURE 16 Comparison of CO emissions of both blend generations with respect to injection timing. SF1 data courtesy of Ran et al. [20].

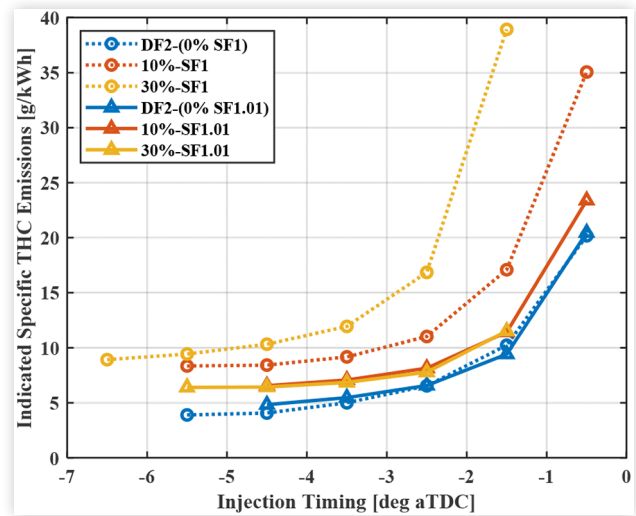


which shows the THC emissions for all blends of both generations. Once again, the emissions of the SF1.01 blends are very close to pure diesel and much lower than the SF1 blends. The explanation for the trends observed in these two figures is that these emissions are inversely proportional to the combustion efficiency, given that CO and THC are products of incomplete combustion. Therefore, the higher combustion efficiency observed in [Figure 14](#) leads to lower levels of CO and THC.

Summary/Conclusions

The findings presented in the sections above can be summarized by the following statements.

FIGURE 17 Comparison of THC emissions of both blend generations with respect to injection timing. SF1 data courtesy of Ran et al. [20].



- The load recorded for baseline diesel was higher than the SF1.01 blends, but that could be attributed to the difference in the equivalence ratio during the experiments. Once this difference was accounted for, the performance of the blends was very close to that of baseline No.2 diesel fuel.
- The combustion efficiency demonstrated by baseline diesel was marginally higher than that of the SF1.01 blends, which leads to a trend of slightly increased CO and THC emissions as the SF1.01 content in the blends was increased.
- No appreciable trend could be established for the NO_x emissions, as the recorded values were extremely low for all data sets.
- The SF1.01 blends showed improvements on the soot emissions compared to diesel, and the 50% SF1.01 blend ratio (50% SF1.01/DF2) clearly demonstrated the lowest sooting propensity by yielding the lowest PM emissions of all blends.
- Blends containing SF1.01 have a shorter burn duration compared to SF1 blends, which leads to higher peak pressure, higher combustion efficiency, and lower CO and THC emissions.
- SF1.01 blends featuring decalin/butylcyclohexane naphthenic content performed closer to baseline No.2 diesel than SF1 blends, which featured only decalin naphthenic content. Thus, butylcyclohexane is more desirable from a combustion performance and emissions characteristic than decalin for the composition of naphthenic content.

Overall, it is concluded that SF1.01 can be blended with No.2 diesel fuel up to 50% by vol. which has been demonstrated to lead to a slight decrease in the power output, as well as yielding slightly higher CO and THC emissions, but showing a significant reduction in the PM emissions.

Acknowledgments

This work was performed at Stony Brook University as part of a CO-OPTIMA project funded by the United States Department of Energy, Energy Efficiency & Renewable Energy, award number DE-EE0008481.

References

- Prakash, R., Singh, R.K., and Murugan, S., "Experimental Studies on a Diesel Engine Fueled With Wood Pyrolysis Oil Diesel Emulsions," *International Journal of Chemical Engineering and Applications* 2 (2011): 395-399. <https://doi.org/10.7763/ijcea.2011.v2.141>.
- Shrivastava, P., Nath Verma, T., and Pugazhendhi, A., "An Experimental Evaluation of Engine Performance and Emission Characteristics of CI Engine Operated with Roselle and Karanja Biodiesel," *Fuel* 254 (2019): 115652. <https://doi.org/10.1016/j.fuel.2019.115652>.
- Subramaniam, M., Solomon, J.M., Nadanakumar, V., Anaimuthu, S. et al., "Experimental Investigation on Performance, Combustion and Emission Characteristics of DI Diesel Engine Using Algae as a Biodiesel," *Energy Reports* 6 (2020): 1382-1392. <https://doi.org/10.1016/j.egy.2020.05.022>.
- Laesecke, J., Ellis, N., and Kirchen, P., "Production, Analysis and Combustion Characterization of Biomass Fast Pyrolysis Oil - Biodiesel Blends for Use in Diesel Engines," *Fuel* 199 (2017): 346-357. <https://doi.org/10.1016/j.fuel.2017.01.093>.
- Cho, S.M., Kim, J.H., Kim, S.H., Park, S.Y. et al., "A Comparative Study on the Fuel Properties of Biodiesel from Woody Essential Oil Depending on Terpene Composition," *Fuel* 218 (2018): 375-384. <https://doi.org/10.1016/j.fuel.2018.01.021>.
- Torri, I.D.V., Paasikallio, V., Faccini, C.S., Huff, R. et al., "Bio-Oil Production of Softwood and Hardwood Forest Industry Residues through Fast and Intermediate Pyrolysis and Its Chromatographic Characterization," *Bioresource Technology* 200 (2016): 680-690. <https://doi.org/10.1016/j.biortech.2015.10.086>.
- Amin, A., "Review of Diesel Production from Renewable Resources: Catalysis, Process Kinetics and Technologies," *Ain Shams Engineering Journal* 10 (2019): 821-839. <https://doi.org/10.1016/j.asej.2019.08.001>.
- Mohan, D., Pittman, C.U., and Steele, P.H., "Pyrolysis of Wood/Biomass for Bio-Oil: A Critical Review," *Energy & Fuels* 20 (2006): 848-889. <https://doi.org/10.1021/ef0502397>.
- Fermoso, J., Pizarro, P., Coronado, J.M., and Serrano, D.P., "Advanced Biofuels Production by Upgrading of Pyrolysis Bio-Oil," *WIREs Energy and Environment* 6 (2017): e245. <https://doi.org/https://doi.org/10.1002/wene.245>.
- Lee, S., Kim, T., and Kang, K., "Performance and Emission Characteristics of a Diesel Engine Operated with Wood Pyrolysis Oil," *Proceedings of the Institution of Mechanical Engineers, Part D: Journal of Automobile Engineering* 228 (2013): 180-189. <https://doi.org/10.1177/0954407013502951>.
- Mueller, C.J., "The Feasibility of Using Raw Liquids from Fast Pyrolysis of Woody Biomass as Fuels for Compression-Ignition Engines: A Literature Review," *SAE Int. J. of Fuels and Lubricants* 6 (2013): 251-262. <https://doi.org/https://doi.org/10.4271/2013-01-1691>.
- Shihadeh, A. and Hochgreb, S., "Diesel Engine Combustion of Biomass Pyrolysis Oils," *Energy & Fuels* 14 (2000): 260-274. <https://doi.org/10.1021/ef990044x>.
- Frijo, S., Gentili, R., Tognotti, L., and Zanforlin, S., "Feasibility of Using Wood Flash-Pyrolysis Oil in Diesel Engines," SAE Technical Paper 982529 (1998). <https://doi.org/https://doi.org/10.4271/982529>.
- Iisa, K., French, R.J., Orton, K.A., Dutta, A. et al., "Production of Low-Oxygen Bio-Oil via Ex Situ Catalytic Fast Pyrolysis and Hydrotreating," *Fuel* 207 (2017): 413-422. <https://doi.org/10.1016/j.fuel.2017.06.098>.
- Mante, O.D., Dayton, D.C., Gabrielsen, J., Ammitzboll, N.L. et al., "Integration of Catalytic Fast Pyrolysis and Hydroprocessing: A Pathway to Refinery Intermediates and 'Drop-in' Fuels from Biomass," *Green Chemistry* 18 (2016): 6123-6135. <https://doi.org/10.1039/C6GC01938B>.
- Agblevor, F.A., Elliott, D.C., Santosa, D.M., Olarte, M.V. et al., "Red Mud Catalytic Pyrolysis of Pinyon Juniper and Single-Stage Hydrotreatment of Oils," *Energy & Fuels* 30 (2016): 7947-7958. <https://doi.org/10.1021/acs.energyfuels.6b00925>.
- Dayton, D.C., Carpenter, J.R., Kataria, A., Peters, J.E. et al., "Design and Operation of a Pilot-Scale Catalytic Biomass Pyrolysis Unit," *Green Chemistry* 17 (2015): 4680. <https://doi.org/10.1039/c5gc01023c>.
- Bittner, J.D. and Howard, J.B., "Role of Aromatics in Soot Formation," in *Conf. Prog. Astronaut. Aeronaut, United States, 7709228*, 62, 1978.
- Azetsu, A., Sato, Y., and Wakisaka, Y., "Effects of Aromatic Components in Fuel on Flame Temperature and Soot Formation in Intermittent Spray Combustion," *SAE Transactions* 112 (2003): 1753-1762. <http://www.jstor.org/stable/44742394>.
- Ran, Z., Hadlich, R.R., Yang, R., Dayton, D. et al., "Experimental Investigation of Naphthenic Biofuel Surrogate Combustion in a Compression Ignition Engine," *Fuel* 312 (2022): 122868. <https://doi.org/10.1016/j.fuel.2021.122868>.
- Ickes, A.M., "Fuel Property Impact on a Premixed Diesel Combustion Mode," *PhD diss.*, University of Michigan, 2009.
- Hariharan, D., Boldaji, M.R., Ziming, Y., Mamalis, S. et al., "Single-Fuel Reactivity Controlled Compression Ignition through Catalytic Partial Oxidation Reformulation of Diesel Fuel," *Fuel* 264 (2020): 116815. <https://doi.org/10.1016/j.fuel.2019.116815>.
- Ran, Z., Longtin, J., Assanis, D., "Investigating Anode Off-Gas Under Spark-Ignition Combustion for SOFC-ICE Hybrid Systems," *International Journal of Engine Research*, 146808742110169, 2021. <https://doi.org/10.1177/14680874211016987>.

24. Ran, Z., Assanis, D., Hariharan, D., and Mamalis, S., "Experimental Study of Spark-Ignition Combustion Using the Anode Off-Gas from a Solid Oxide Fuel Cell," SAE Technical Papers 2020-01-0351 (April 14, 2020). <https://doi.org/10.4271/2020-01-0351>.

Contact Information

Rodrigo Ristow-Hadlich, Graduate Student Research Assistant,
Dept. of Mechanical Engineering, Stony Brook University,
118 Advanced Energy Center (AERTC),
1000 Innovation Rd,
Stony Brook,
NY 11794,
USA,
rodrigohadlich@gmail.com

Prof. Dimitris Assanis, Assistant Professor,
Dept. of Mechanical Engineering, Stony Brook University,
131 Light Engineering,
100 Nicholls Rd,
Stony Brook,
NY 11794,
USA,
dimitris.assanis@stonybrook.edu

Definitions/Abbreviations

acc. - Accuracy
bTDC - Before Top Dead Center
CAD - Crank Angle Degree
CO - Carbon Monoxide
CO₂ - Carbon Dioxide
CFP - Catalytic Fast Pyrolysis
DF2 - Diesel Fuel 2 (research grade)
HDO - Hydrodeoxygenation
HT - Hydrotreating
IMEP_{gross} - Gross Indicated Mean Effective Pressure
NO_x - Nitrogen Oxide
PM - Particulate Matter
pre. - Precision
res. - Resolution
RSS - Root Sum of Squares
SF - Surrogate Fuel
SOI - Start of Injection
TDC - Top Dead Center
THC - Total Hydrocarbons